Calibration of Submerged Radial Gates

A. J. Clemmens, M.ASCE[1]; T. S. Strelkoff, M.ASCE[2]; and J. A. Replogle, F.ASCE[3]

Abstract: Calibration equations for free-flowing radial gates typically provide sufficient accuracy for irrigation district operations. However, many water purveyors have difficulty in determining accurate discharges when the downstream water level begins to submerge the gate. Based on experimental laboratory studies, we have developed a new calibration method for free-flowing and submerged radial gates that allows for multiple gates and widely varying upstream and downstream channel conditions. The method uses the energy equation on the upstream side of the structure and the momentum equation on the downstream side, and thus is called the Energy-Momentum Method. An iterative solution is required to solve these two equations, but this allows calibration from free flow to submerged flow continuously through the transition. Adjustments to the energy equation for free flow are described, along with an additional energy adjustment for the transition to submerged flow. An application is used to describe the new procedure and how it overcomes the limitations of current energy-based methods.

DOI: 10.1061/(ASCE)0733-9429(2003)129:9(680)

CE Database subject headings: Gates; Flow measurement; Hydraulic jets; Hydraulic jumps; Calibration.

Introduction

Radial gates are a common water control structure in much of the western United States. Their advantage over vertical sluice gates is that the lifting force is minimal. The U.S. Bureau of Reclamation has used radial gates as a standard structure for nearly a century. They are also used in private irrigation projects, and in projects of the U.S. Army Corp of Engineers. These structures are pervasive in canals or regulated streams in the central and western United States.

Calibration methods for free-flowing radial gates are available in standard references and have been used with reasonable success to measure flow (Henderson 1966; Bos 1989). Calibration of submerged flows have had mixed success, with errors up to 50% reported in some cases. These calibration methods are based exclusively on the energy equation. Some use the momentum equation to define the limit between submerged and free flow. However, a major flaw with all these methods is that they are all based on upstream and downstream channels that are rectangular with a width the same as the gate, and typically have the same floor elevation. This rarely occurs in practice. Where multiple gates occur, submerged calibration has proven successful only when all gates are open the same amount and their total width is similar to the width of the downstream channel (e.g., at the head of the All American Canal in Southern California).

In 1999, we conducted a study on the calibration of radial gates in the hydraulics laboratory of the U.S. Water Conservation Laboratory. Details of the experimental setup are provided in a later section. In this paper, we present a solution method for submerged radial gates that uses the energy equation on the upstream side of the gate (the same as for free flow) and the momentum equation on the downstream side. A new transition between submerged and free flow is defined as an adjustment to the energy equation.

Theory

Free Flow

The calibration of flow under a vertical sluice gate is a classic problem in hydraulic engineering and has been studied for more than a century (e.g., von Helmholtz 1868). Montes (1997) provides an excellent summary of the theoretical and experimental studies that have been conducted under free-flow conditions (i.e., not influenced by downstream water depth). However, the discussion of Montes' article by Speerli and Hager (1999) and by Webby (1999), along with Montes' (1999) closure, suggest that our theoretical understanding of even free-flowing sluice gates is incomplete. For practical application, the errors associated with these disagreements in theory are relatively small, being at most $\pm 5\%$. Many gates contain a J-seal at the lip to allow the gate to seal when it is closed. This alters the calibration by more than these theoretical discrepancies. Thus, field calibrations are often used, which side-steps these theoretical details. However, the research on submerged flow reported herein relies on the free-flow theory, thus it is worth further discussion.

The complexity of the problem stems from our inability to theoretically determine the free surface configuration downstream from the gate, even in free flow. The jet emanating from under the gate reaches a minimum depth at the vena contracta (Section 2 in Fig. 1). The theoretical difficulties are associated with defining

[1]Laboratory Director, U.S. Water Conservation Laboratory, USDA-ARS, 4331 E. Broadway, Phoenix, AZ 85040. E-mail: bclemmens@uswcl.ars.ag.gov

[2]Research Hydraulic Engineer, U.S. Water Conservation Laboratory, USDA-ARS, 4331 E. Broadway, Phoenix, AZ 85040. E-mail: fstrelkoff@uswcl.ars.ag.gov

[3]Research Hydraulic Engineer, U.S. Water Conservation Laboratory, USDA-ARS, 4331 E. Broadway, Phoenix, AZ 85040. E-mail: jreplogle@uswcl.ars.ag.gov

Note. Discussion open until February 1, 2004. Separate discussions must be submitted for individual papers. To extend the closing date by one month, a written request must be filed with the ASCE Managing Editor. The manuscript for this paper was submitted for review and possible publication on June 25, 2002; approved on March 19, 2003. This paper is part of the ***Journal of Hydraulic Engineering***, Vol. 129, No. 9, September 1, 2003. ©ASCE, ISSN 0733-9429/2003/9-680–687/$18.00.

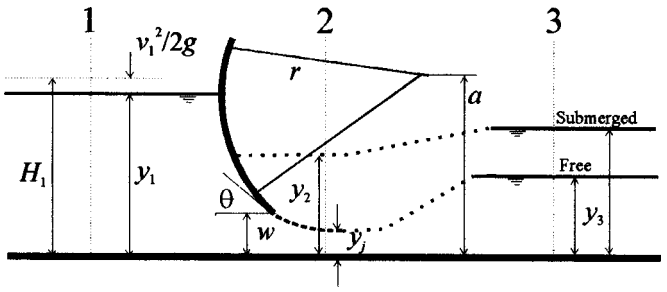

Fig. 1. Definition sketch for radial gate

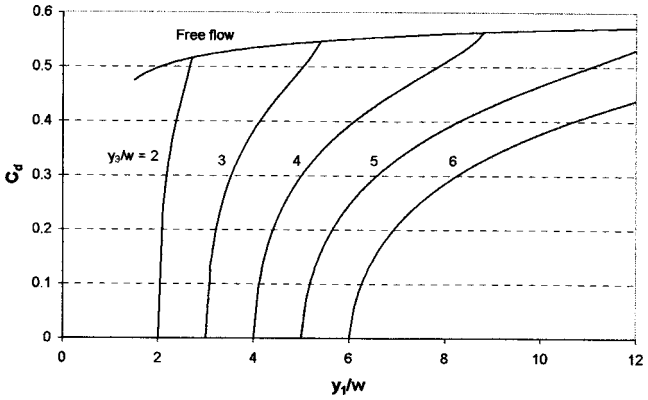

Fig. 2. Vertical sluice gate discharge coefficients for free and submerged flow (after Henry 1950 and Swamee 1992). Similar curves for radial gates vary with gate dimensions.

the contraction coefficient δ (ratio of minimum depth y_j to gate opening w) for the variety of flow configurations encountered. In general, the contraction coefficient varies with the angle of the gate θ. Results shown later suggest that the contraction coefficient is not significantly influenced by the ratio of gate opening to upstream energy head w/H_1.

If we apply the energy equation between Section 1 (see Fig. 1) upstream from the gate (rectangular channel with the same width as the gate) and the vena contracta, assuming no energy losses and no downstream influence, we get

$$H_1 = y_1 + \frac{q^2}{2gy_1^2} = y_j + \frac{q^2}{2gy_j^2} = \delta w + \frac{q^2}{2g(\delta w)^2} \tag{1}$$

where H_1 = upstream energy head; y_1 = upstream water depth; q = discharge per unit width of gate and channel; $y_j = \delta w$ is the depth at the vena contracta or minimum jet thickness; and g = acceleration of gravity. The discharge for a rectangular channel $Q = qb_c$. Substituting this relationship into Eq. (1) and solving for discharge results in

$$Q = C_d w b_c \sqrt{2gy_1} \tag{2}$$

where b_c = width of the gate and C_d = discharge coefficient. An expression for C_d can be derived from Eqs. (1) and (2), namely (Bos 1989)

$$C_d = \frac{\delta}{\sqrt{1 + \delta w/y_1}} \tag{3}$$

This equation applies to both vertical sluice gates and radial gates, the primary difference being the value of the contraction coefficient.

Two approaches can be used to solve Eq. (2) for discharge when the upstream water depth, gate opening, and width are known. In one, a value for C_d is read from a graph (e.g., Fig. 2) or computed from an equation fit to laboratory data. For vertical sluice gates, this discharge coefficient is a function of the relative gate opening w/H_1, or w/y_1 as shown in Eq. (3). Such graphs are commonly recommended (Henry 1950; Rajaratnam and Subramanya 1967b; Buyalski 1983; Bos 1989). Alternatively, δ is found from a table or equation and C_d computed from Eq. (3) (Bos 1989). Not surprisingly, the empirical relationships for C_d provide more accurate estimates of discharge than do measured contraction coefficients and Eq. (3). Montes (1997) summarizes the theoretical work that has gone into the determination of the contraction coefficient and the reasons why the contraction coefficient, alone, is insufficient to determine the discharge coefficient. Most of his research dealt with flat sluice gates, either vertical or inclined. Montes found that the contraction coefficient was strongly influenced by the gate angle (for the case of radial gates, the angle of the gate lip θ, where the water surface becomes free). He suggested that the discrepancy in the prediction of discharge with the contraction coefficient was primarily due to energy losses in the upstream channel as the flow approached the gate. The development of boundary layers on the floor below the gate and on the gate face could not explain all of the differences found. Webby (1999) disagreed with Montes' conclusion that energy loss exists upstream from the gate, comparing field measurements with theoretical predictions of the contraction coefficient by Isaacs and Allen (1994). Insufficient data were provided on these field trials to judge their accuracy. Speerli and Hager (1999) present support for the notion of energy losses, showing clear pictures of eddies and vortices. However, to date no one has proposed a method for estimating the actual energy loss. While much of this discussion is for vertical sluice gates, the same issues apply to radial gates.

For this study of radial gates, we propose an energy equation based on the jet velocity head, as follows:

$$H_1 = H_j + \Delta H = y_j + \alpha_j \frac{v_j^2}{2g} + \xi \frac{v_j^2}{2g} \tag{4}$$

where H_j = energy head at the vena contracta; α_j = velocity distribution coefficient; and ξ = energy loss coefficient. Experimentally, we cannot separate the effects of jet velocity distribution, reflected by α_j, from our energy loss term, reflected by ξ. For simplicity, we will assume $\alpha_j = 1$. Any deviation from unity by α_j will end up in ξ, giving a combined coefficient. As with other hydraulic structures, this energy loss coefficient is expected to be a function of the Reynolds number.

Since the discharge is equal to velocity times area, in the jet we have $Q = \delta w b_c v_j$. Substituting for v_j and y_j in Eq. (4) and solving for discharge gives

$$Q = \delta w b_c \sqrt{\frac{2g(H_1 - \delta w)}{1 + \xi}} \tag{5}$$

For a given geometry, this provides a relationship between discharge and upstream energy head, with only the contraction coefficient δ and the loss coefficient ξ to be evaluated.

This differs substantially from prior solutions of the radial-gate energy equation in several ways. First, it is expressed in terms of upstream energy head rather than depth. This allows one to have an upstream velocity head that is not related to the flow in any one gate, as assumed in Eq. (2), for example when multiple gates and weirs are used. Second, it includes an energy loss term rather than relying on empirical discharge coefficients. And finally, the

contraction coefficient is not buried in the discharge coefficient. These differences allow us to determine the head-discharge relationships for a wider range of conditions than other methods.

Submerged Flow

Only a few studies on submerged radial gates are available in the literature. The most common approach has been to use an empirical discharge coefficient according to the amount of submergence. This approach was suggested by Henry (1950) and Rajaratnam and Subramanya (1967b) for vertical sluice gates and used by Buyalski (1983) for radial gates. One difficulty with this approach is that the curves are very steep, resulting in a large change in discharge coefficient for a small change in upstream depth or gate opening. Another approach (Bos 1989) is to use the same discharge coefficient as for free flow, but with the water level difference across the gate replacing the upstream depth. A challenge with this approach is to determine when to use the upstream head and when to use the head differential. The standard textbook approach is to use the conjugate depth equation for a rectangular channel to determine whether or not the gate is submerged [e.g., as suggested by Bos (1989)].

These approaches have a major flaw when applied to practical situations. All of the studies and the conjugate depth relationship assume that the downstream channel is of the same cross section as the gate. The calibration results are highly dependent upon this condition, and the assumed condition is rarely found in practice. The current approaches cannot easily deal with these real-world conditions.

Where a hydraulic jump occurs, energy losses are difficult, if not impossible, to predict. This usually requires solution of the momentum equation. However, it is also not practical to solve the momentum equation from the upstream section to the downstream section since the forces on the gate are unknown. Instead, we propose to use the energy equation from the upstream side to the vena contracta, where we think we can capture the essential flow conditions, and the momentum equation from the vena contracta to the downstream section. Under normal operation, the depth and velocity at the vena contracta will not be measured. Instead, those conditions must be inferred from the equations.

Application of the energy and momentum equations to submerged flow conditions assumes that the jet thickness essentially remains constant. Such results were found by Rajaratnam and Subramanya (1967a), among others. To date, no one has questioned the validity of this assumption during initial submergence, although it is well recognized that calibrations under such conditions are problematic. However, measurement of velocity distributions within hydraulic jumps (Rajaratnam 1965a, b; Narayanan 1975; and Gunal and Narayanan 1996) show a decreasing jet velocity with distance into the jump, exhibiting a deceleration entirely in keeping with the adverse pressure gradient, the increasing depth within the jump, and distance from the toe. In fact, the flow just downstream from the gate, as y_2 is increased, comprises an incomplete jump gradually approaching the classical wall jet (Rouse et al. 1959), and finally a standard wall jet with the jet similar in configuration to the jet under free flow. Thus the jet goes from its free-flow thickness to something wider, and then back to its free-flow thickness as it goes from free to partially submerged to highly submerged.

Numerical modeling of this behavior during initial submergence between Sections 1 and 2 with the energy equation requires a reduction in jet velocity, and for a constant discharge, an expansion in the jet thickness [as suggested by Tel (2000)]. In a simpler, and ultimately equivalent procedure, we postulate a kinetic energy correction term E_{corr} for the transition zone, such that the energy equation becomes

$$H_1 = y_2 + \frac{v_j^2}{2g} + \xi \frac{v_j^2}{2g} - E_{\text{corr}} \tag{6}$$

in which the subscript j refers to the "live stream" conditions in the jet at the vena contracta and the subscript 2 refers to the vena contracta location, whether free or submerged. In this relationship, v_j is set to $Q/b_c y_j$, with y_j remaining at the free-flow value, δw. The nature of this energy correction is presented in a later section. Solving Eq. (6) for discharge yields

$$Q = \delta w b_c \sqrt{\frac{2g(H_1 - y_2 + E_{\text{corr}})}{1+\xi}} \tag{7}$$

The solution of Eq. (6) for submerged discharge requires, in addition to what is needed for free flow in Eq. (2), an estimate of the energy correction E_{corr} and an estimate for the depth y_2 at the vena contracta. This depth is extremely difficult to measure in the field. The flow there is highly turbulent and "*frothy*" such that a surface measurement is insufficient to determine the true depth (i.e., as reflected in the pressure below the surface) and accurate wall-pressure taps are difficult to construct for such high velocity flows. This depth is not currently measured in the field. Instead, the water depth in the downstream channel y_3 is measured. To utilize the measured depth y_3 instead of y_2, a momentum relationship between Sections 2 and 3 is introduced.

Conservation of momentum, applied from the vena contracta to Section 3, can be written as

$$Q v_e + b_c g \frac{y_2^2}{2} + \frac{F_w}{\rho} = Q v_3 + \frac{F_3}{\rho} \tag{8}$$

where v_e = effective velocity in the jet (discussed below); v_3 = downstream velocity; ρ = density of water (mass per unit volume); F_3 = hydrostatic-pressure force exerted by the downstream water depth; and F_w = component of the force of water on all surfaces between Sections 2 and 3 in the direction of flow, including hydrostatic forces on all walls. These surfaces can be determined by taking the downstream area and projecting it back to Section 2 (assuming the section only expands from Section 2 to Section 3). Projected surfaces include the edges of the piers that separate the individual gates, closed gates, weir overfall sections, and the canal walls where the cross section expands. For rectangular cross sections, the force terms reduce to $bgy^2/2$, with subscripts 3 or w on b and y. For the short distances involved here, we can ignore the channel friction and bed slope effects.

Eqs. (7) and (8) represent solutions for flow on the upstream and downstream sides of the vena contracta, with Q and y_2 unknown, and the rest derivable from the measured water depths, gate opening, cross-section shapes, and empirical relationships for δ, and ξ, and E_{corr}.

Simultaneous solution of these two equations is referred to here as the energy-momentum (E-M) method. Application of this method is complicated by (1) quantification of the energy loss coefficient ξ; (2) application of the energy equation under slightly submerged conditions (i.e., E_{corr}); and (3) estimation of the wall forces for application of the momentum equation. The force on the walls is assumed to be based on a water depth there—hypothesized to be between the depths at Sections 2 and 3. The effective water depth at the walls is found as the weighted average of these two depths, with weighting coefficient p

$$y_w = py_3 + (1-p)y_2 \quad (9)$$

Laboratory experiments were performed to develop the necessary relationships and to test the applicability of these equations.

Experimental Setup

A model radial gate structure provided by the Salt River Project (SRP) was used to conduct these experiments. The gate-lip seals were removed for the experiments so that we could make sure that we could properly model the phenomenon without the seals. New side walls were constructed for the gate since those provided by SRP were broken and did not match our channel. The 4-ft (1.23 m) wide 2-ft (0.61 m) high glass-sided flume at the U.S. Water Conservation Laboratory was used to perform these tests. The flume is 15.2 m long, of which only a small part was needed for these tests. Water was supplied from a constant head tank and discharges were weighed in a large weigh-tank and scale system. The head-tank, flume and weigh-tank system has a capacity of 500 L/s, although this model was capable of handling only about 60 L/s.

The radial gate is 0.457 m wide and has a radius of 0.457 m. The gate is set between two side walls that are 1.219 m long. The trunnion-pin height is set at 0.366 m, and is placed 0.091 m upstream from the downstream end of the side walls, which, if scaled, is typical of SRP installations. An entrance transition was constructed to avoid a blunt entry into the gate structure, since the gate width is less than half of the flume width. This entrance has a radius of 0.39 m. The upstream and downstream water levels were measured at distances 3.5 m upstream and 7.59 m downstream from the gate trunnion, respectively. The water levels, velocities, and energy heads for Section 2 were measured at a distance from the gate lip of two times the gate opening, the approximate location of the vena contracta.

The upstream water level was measured with a point gauge. The downstream water levels at Sections 2 and 3 were measured with the static side of a 5 mm-diameter Prandtl tube which was placed in the middle of the stream. The depth of water at Section 2 under free-flow conditions was also measured with a point gauge. Velocity distributions at Section 2 were measured with a 2 mm-diameter Prandtl tube. All water levels and pressures were registered to the invert elevation immediately under the gate.

For the free-flow experiments, the gate position was set and accurately measured. Then flow was turned on and a discharge set. Once the flow stabilized, the water-level and velocity measurements were made, and discharge measurements were taken with an 30,000 L (8,000 gallon) weight tank system which is typically accurate to 0.1%. Then the flow is set to a new discharge and the process repeated. The range of discharge for each gate opening was determined at a minimum, to provide orifice flow, and at a maximum, to avoid overtopping. Free-flow tests were run at gate openings of 0.0381, 0.0762, 0.1143, 0.1524, and 0.1905 m.

For the submerged-flow experiments, the gate position was set and measured. The flow was turned on and set with free flow emerging from under the gate. Water level and discharge measurements were taken. Then a gate downstream from the y_3 measurement site was raised, gradually, until the upstream water level increased by 1 mm. This was judged to be the start of submergence. All water levels were measured, as was the discharge, once flow had stabilized. After these measurements, the downstream gate was raised a small amount and the process repeated. The number of water levels for which submerged flow was measured varied from 6 to 9 for each discharge. However in all cases, the tests were run until the gate was fully submerged. Submerged flow data were collected for only one gate position, $w = 0.0762$ m.

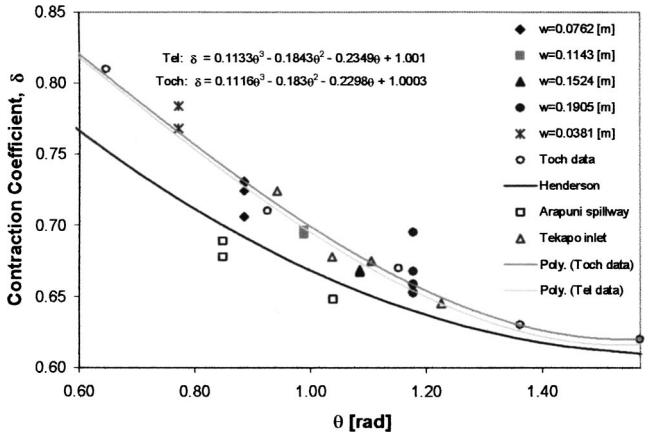

Fig. 3. Radial gate contraction coefficient δ as function of gate angle θ

In this study, the contraction coefficients were found by measuring the gate opening and measuring the pressure in the jet at the vena contracta with a Prandtl tube roughly in the center of the jet. For several runs, we measured the pressure distribution within the jet and it was sufficiently hydrostatic, verifying that our single pressure readings were sufficient to define the contraction coefficient.

Results

Free Flow

Fig. 3 shows the values of δ from this experiment and from prior studies, as a function of the angle of the gate lip θ. These data suggest the following relationship [reported by Tel (2000)]:

$$\delta = 1.001 - 0.2349\theta - 0.1843\theta^2 + 0.1133\theta^3 \quad (10)$$

where $\theta = \arccos(\{a\text{-}w\}/r)$ expressed in radians; r = radial gate radius; and a = gate trunnion-pin height (height of gate pivot point above invert). The data from the current study (originally reported by Tel) essentially confirms the relationship of Toch (1955). We found essentially no influence of w/H_1 on the contraction coefficient.

This is consistent with most of the experimental data presented by Montes (1997) and with some theoretical results, such as Fangmeier and Strelkoff (1968). But it is in contrast to many of the theoretical studies, particularly Isaacs and Allen (1994). The field data of Webby (1999) is varied, with one site in agreement with Toch (Tekapo Inlet) and another which shows a large discrepancy (Arapuni Spillway). At this point, we trust the laboratory data over the theoretical predictions and field data, although more laboratory data would be useful to support this. The data in Fig. 3 do not support the recommendation of Bos (1989) to use Henderson's equation (Henderson 1966).

Velocity profile measurements under free flow showed that the velocity distribution coefficient α_j varied between 1.01 and 1.03. This value is influenced by the drag on the walls, which is expected to be relatively less for the prototype than for the scale model. However, since values of ξ are much larger, we combined these two for further analysis below, and expressed this as 1

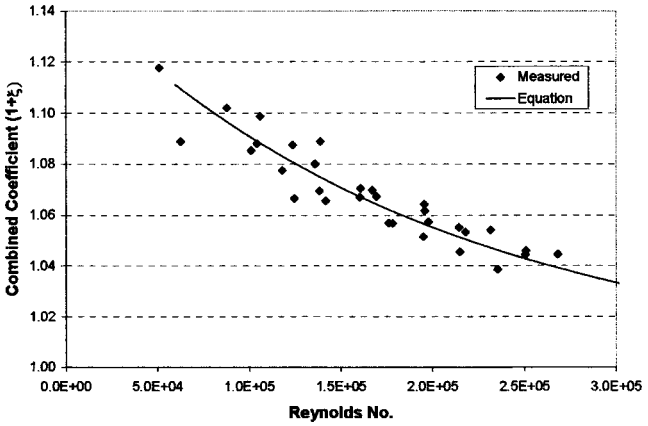

Fig. 4. Combined velocity distribution and energy coefficient as a function of entrance Reynolds number for free flowing radial gate

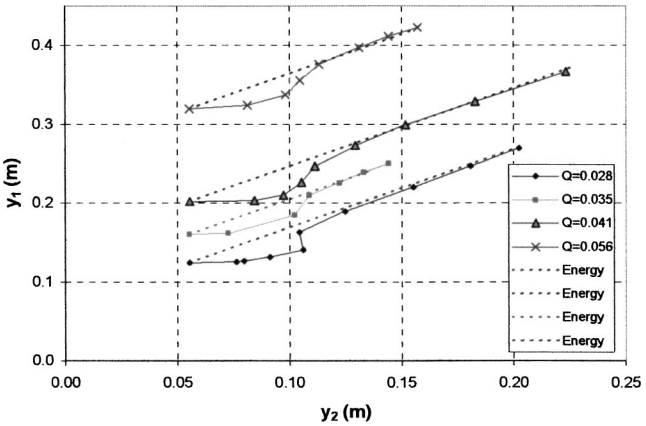

Fig. 6. Preliminary application of energy equation from upstream side of radial gate structure to vena contracta (flows in m^3/s)

$+\xi$, where α_j has been set to unity. The combined coefficient is shown in Fig. 4, which shows values ranging from 1.04 to 1.12. An equation was fit to the data, which has the combined coefficient approaching 1.0 as the Reynolds number approaches infinity. The Reynolds number used here R was defined as the velocity (unit width discharge divided by gate opening) times the hydraulic radius just upstream from the gate (area over wetted perimeter for upstream water depth immediately upstream from the gate, i.e., within gate piers) divided by the kinematic viscosity. Other ways to express the Reynolds number were tested, but this provided the best fit (highest correlation) or least scatter in the results. The resulting relationship is

$$1+\xi=1+0.15e^{-5\times10^{-6}\mathrm{R}} \tag{11}$$

Of note is that the energy loss for this scale model is highly dependent upon the Reynolds number. This is consistent with our previous research on critical depth flumes, where energy losses were related to the Reynolds number (Replogle 1975; Bos et al. 1984; Clemmens et al. 2001). Of significance to this research is that these energy losses are relatively high for laboratory models where Reynolds numbers are low. For prototype gates, Reynolds numbers may be an order of magnitude higher. Extrapolation of the results presented in Fig. 4 would suggest energy losses for field-scale gates on the order of 1 or 2% and not strongly influenced by Reynolds numbers. This may explain the discrepancy between the laboratory results reported by Montes (1997) and the field data reported by Webby (1999).

Solution of Eq. (5) with the coefficients from Eqs. (10) and (11) (Figs. 3 and 4) agreed with laboratory data to within about 1% in all but a few cases (Fig. 5). The large spread in error resulted from data at one particular gate opening, suggesting a minor problem with measurements taken for that gate opening. Otherwise, errors were within $\pm1\%$.

Submerged Flow

From Eq. (6) without the correction term, one might expect a nearly linear relationship between y_1 and y_2 for a constant discharge. However, laboratory results differ substantially from this result, as shown in Fig. 6. At high submergence, this relationship looks reasonable, suggesting that the jet is the same size as under free flow, only submerged. Tel (2000) suggested adjusting the energy equation by adjusting the jet thickness, but a useful relationship could not be found.

We solved Eq. (6) for E_{corr} with the measured values of Q, y_1, and y_2, and with ξ from the free-flow tests. The resulting energy correction relative to the change in depth at the vena contracta $[E_{\mathrm{corr}}/(y_2-y_j)]$ is shown in Fig. 7 as a function of this change in depth relative to the free-flow jet thickness $[(y_2-y_j)/y_j]$. The consistency of the relationship shown in Fig. 7 for different discharges (and w/H_1 values) is encouraging. It essentially says that

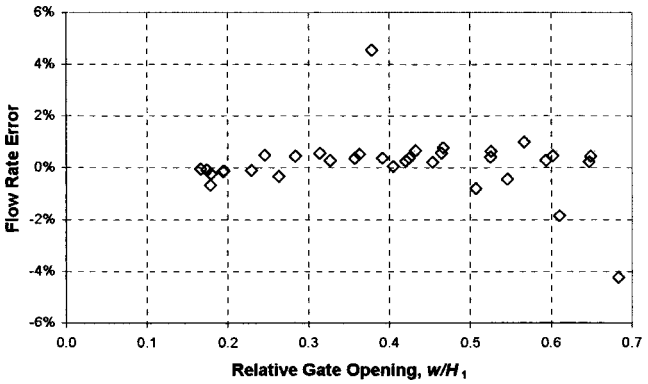

Fig. 5. Accuracy of radial gate free-flow discharge computed with energy equation and curve fits for contraction coefficient and energy loss coefficient

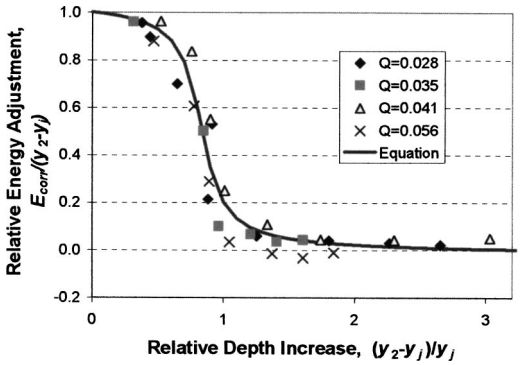

Fig. 7. Relative energy adjustment required to apply free-flow energy equation to submerged flow for a radial gate up to vena contracta (flows in m^3/s)

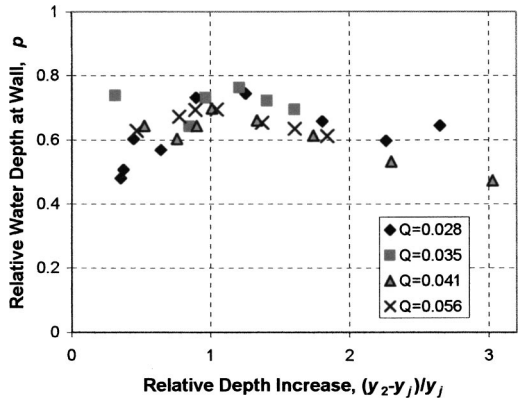

Fig. 8. Weighting coefficient p for water depth on back wall of radial gate structure (flows in m^3/s)

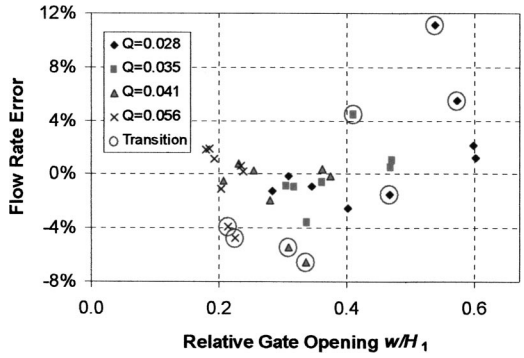

Fig. 9. Error in discharge computed with the energy-momentum method as function of relative gate opening (flows in m^3/s)

for small submergence depths, the contribution of that depth increase to the apparent increase in energy at Section 2 is small (i.e., almost 100% of the depth increase is canceled with E_{corr}). Here, the low depth over the high-speed jet behaves essentially like a hydraulic jump to slow the jet down. When the jet becomes highly submerged, the adverse pressure gradient typical of the jump vanishes, and the thickness of the jet essentially returns to its original value. Thus the behavior shown in Fig. 7 is entirely reasonable. While the partial jump is in effect, increases in tail water elevation have almost no effect on upstream water level. But as the ''wall-jet'' condition is approached, further increases in tailwater depth produce corresponding upstream depth changes. The fitted equation for the relationship in Fig. 7 is

$$E_{\text{corr}} = (y_2 - y_j)\left(0.52 - 0.34 \arctan\left\{7.89\left[\frac{y_2 - y_j}{y_j}\right] - 0.83\right\}\right) \tag{12}$$

which we restrict to values between 0 and 1. This relationship essentially describes the transition from free to fully submerged flow, and allows us to compute flow continuously through the transition zone without changing equations.

An equivalent jet velocity for use in the momentum equation was determined by replacing the second and fourth terms on the right-hand side of Eq. (6)

$$\frac{v_e^2}{2g} = \frac{v_j^2}{2g} - E_{\text{corr}} \tag{13}$$

The equivalent velocity then replaces the jet velocity in momentum Eq. (8), since this effective velocity more accurately reflects the actual momentum. This formulation leaves the computed upstream energy loss unchanged, except with Reynolds number (which changes with discharge and upstream depth as the gate becomes submerged).

The measured data were used to compute the coefficient p for the effective wall pressure from Eqs. (8) and (9) assuming hydrostatic pressure distributions, as shown in Fig. 8. While there was some scatter in the data, a strong trend was not apparent. For the remaining analysis, an average value of 0.643 was used.

At this point, some verification of the relationships was attempted. The energy and momentum equations [Eqs. (7) and (8)] were solved with only knowledge of the upstream and downstream water levels and the gate opening and dimensions. The relationships in Eqs. (10) through (13) (Figs. 3, 4, and 7) were used, along with $p = 0.643$. The resulting errors in discharge are shown in Fig. 9. The circled values are those that fall within the sharp transition range in Fig. 7 (relative energy adjustment values between 0.2 and 0.8). Those within the sharp transition zone have errors that ranged from -8 to $+12\%$, while all the other values are estimated to within -4 to $+3\%$. We also speculate that the relative depth at which the transition shown in Fig. 7 occurs is a function of the ratio w/H_1, although there are not enough data points to define such a relationship (i.e., Fig. 7 would consist of a family of curves).

Discussion

The range of conditions and the accuracy of estimated discharges suggest that the contraction coefficient and energy loss coefficients are sufficiently accurate for free-flow conditions when gate seals are not used. Additional tests are needed to determine the influence of the gate seals on these relationships.

For submerged conditions, further studies are needed to define the energy-correction relationship over a wider range of conditions (e.g., with a range of w/H_1 values). The study reported here used only one gate position. In theory, this does not pose a limitation. However, further experiments at other gate positions would determine whether or not other variables influence the relationships posed. Such studies also might provide enough data to separate the effects of w/H_1 on the energy correction. It is not expected that the use of a gate seal will influence submerged calibration, beyond its influence on free-flow conditions, but this needs to be verified.

Use of the momentum equation under submerged conditions requires an estimate of the backpressure on walls on the downstream side of the check structure. While an average relative value from the tests was used in the analysis presented here, this relative value is likely to vary with the layout of the gates and weirs within a check structure. Application of the E-M method might require refinements in this estimated pressure.

Also, additional studies of submergence are needed at values of w/H_1 above 2/3, a theoretical limit at low submergence, but which can be greatly exceeded at high submergence.

Application

As an example, we provide an application at the Salt River Project (SRP) in Arizona. At some check structures, operators report flow errors as high as 50%. SRP has been using the free-flow [i.e., Eqs. (2) and (3)] and submerged [i.e., Eqs. (2) and (3) with $y_1 - y_3$ replacing y_1 in Eq. (2)] radial-gate calibration

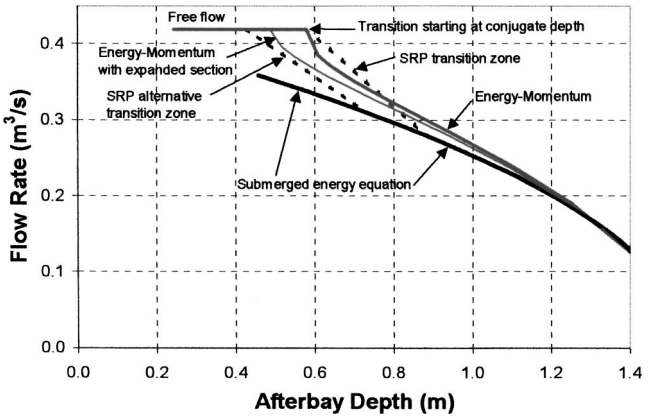

Fig. 10. Radial-gate flow rates computed with energy equation (as used by SRP) and energy-momentum method (fixed gate opening and upstream depth)

method suggested by Bos (1989). Under this method, the gate is assumed to be submerged when the downstream water level reaches the conjugate depth. The specifics of the gate conditions for this example are as follows: gate width, $b_c = 1.22$ m (4 ft); trunnion-pin height, $a = 1.24$ m (4.06 ft); gate radius, $r = 1.52$ m (5 ft); gate radial travel = 0.140 m (0.46 ft); vertical gate opening, $w = 0.087$ m (0.285 ft); forebay water level, $y_1 = 1.54$ m (5.05 ft); and gate angle, $\theta = 0.715$ rad. For their calibration procedures, they use a contraction coefficient, $\delta = 0.733$, which from Eq. (3) gives a free flow discharge coefficient $C_d = 0.718$; and submerged discharge coefficient $C_d = 0.734$. These gates have a stiff rubber music-note seal.

The results of application of Bos' (1989) equations are shown in Fig. 10, where the calibration relationships for a fixed gate and given upstream water level are shown as a function of downstream (afterbay) depth. The horizontal line at the top represents free flow (i.e., not influenced by downstream depth). The far right point of this horizontal line represents the depth conjugate to the free-flowing jet thickness at its vena contracta for a downstream channel of the same width as the gate. The lower heavy line is the energy-based submerged-flow solution, where discharge is proportional to the square root of the head difference.

No recommendation is given on transitioning from the conjugate depth point to the submerged-flow line. A straight drop is implied, but is clearly unreasonable. SRP chose to use a 1 ft (0.3 m) transition zone starting at the conjugate depth, described essentially by a straight (dashed) line, as shown in Fig. 10. In some situations, SRP personnel found that this transition was not providing an appropriate solution. They experimented with another transition, assuming that the one ft (0.3 m) transition zone was centered around the computed conjugate depth. This alternative transition zone is also shown as a dashed line in Fig. 10. Selection of the best transition was by trial and error, and they found that the selection varied from gate to gate and even with flow rate for a given gate.

We applied the proposed energy-momentum (E-M) solution to this situation. In order to match the SRP conditions under free flow for this gate with a gate-lip seal, we used their contraction coefficient of 0.733 and assumed no energy loss (i.e., $1 + \xi = 1.0$). The E-M solution is shown in Fig. 10. As one can see, the SRP transition zone does a reasonable job of matching this transition, although differences of roughly 8% occur. The transition occurs more rapidly at first, when submergence is just started, but then becomes more gradual and only approaches the submerged-energy-equation solution when the gate is highly submerged (approximately twice the conjugate depth).

Many SRP check structures contain multiple gates (e.g., 3 to 5) and often weirs on either side of the gates. SRP does not try to keep all gates at the same opening, and at low flows may have one or more gates closed. Thus the effective width of the downstream channel may be much wider than that of the gates that are open. In this case, the downstream velocity does not reflect conditions on which the energy-based radial-gate equations are based. In particular, the conjugate depth is much lower. The E-M solution was computed for a situation where the downstream channel is twice as wide as the gate. This result is shown in Fig. 10 as the E-M solution with an expanded section. It shows the change in conjugate depth and how that influences the calibration. Eventually the two E-M solutions converge, but again at very high submergence. For tailwater depths in between the two conjugate depths, differences reach roughly 15%. For wider expansions, and thus lower downstream velocities, larger differences are possible.

As can be seen, SRP's alternate transition zone more nearly matches the solution for a downstream channel that is twice as wide as the active gates. Thus the need to have multiple transition zones can be explained entirely by which and how many gates are being used at a site relative to the downstream channel width. Not having all gates at the same position further complicates the situation, since some may be submerged while others are not. The E-M solution provides a method for computing the discharge of each gate at a check structure, even when their submergence conditions differ.

Conclusions

A new method was developed for the calibration of radial gates, called the energy-momentum or E-M method.

- Under free flow, the energy equation is used to determine discharge. The free-flow calibration requires a contraction coefficient and an energy loss coefficient. Equations are provided here for both.
- Under submerged flow, the energy equation is used for the upstream side of the gate (upstream from vena contracta) and the momentum equation is used for the downstream side of the gate (downstream from vena contracta). The point of transition between free and submerged flow is determined by the momentum equation.
- An energy adjustment is required for the energy equation under submerged flow to adjust for the changes in the vena contracta during initial submergence. A rough equation is provided for this transition, but this needs further refinement.
- The momentum equation must account for the hydrostatic forces on the downstream side of the check structure. An approximate method for determining this was provided, but this likely needs refinement.

An example was provided that shows how differences between the downstream channel and gate width affect the gate calibration under submerged flow. The example also contrasts the E-M method with an existing method of applying the energy equation to submerged flow.

Acknowledgments

The writers would like to acknowledge the contributions of Jan Tel and Skip Eshelman who collected the laboratory data. The high quality of this data allowed useful relationships to be developed. Jan Tel also performed some of the preliminary data analyses that ultimately led to the results presented here. The writers would also like to acknowledge the contributions of Robert Gooch and the Salt River Project for supplying the model gate and for providing the example conditions.

Notation

The following symbols are used in this paper:

a = gate trunnion-pin height (height of gate pivot point above invert);
b_c = gate width;
b_w = width of structure walls on downstream side;
C_d = discharge coefficient
E_{corr} = energy correction term;
F_w = component of force of water on all surfaces between Sections 2 and 3 in direction of flow, including hydrostatic forces on all walls;
F_3 = hydrostatic-pressure force exerted by downstream water depth;
g = acceleration of gravity;
H_j = energy head at vena contracta;
H_1 = upstream energy head;
k = kinematic viscosity (1.14×10^{-6} m^2/s)
p = depth weighting coefficient;
Q = discharge;
q = discharge per unit width of gate or channel;
R = Reynolds number$=vR/k$, where $v=Q/b_cw$ and R $=b_cy_1/(b_c+2y_1)$;
r = radial gate radius;
v_e = effective flow velocity for vena contracta under submerged flow;
v_j = average flow velocity at the vena contracta under free flow;
v_1 = average flow velocity upstream from gate;
v_3 = average flow velocity downstream from gate;
w = gate opening;
y_j = water depth at vena contracta under free flow or minimum jet thickness;
y_w = water depth on downstream side of structure walls;
y_1 = upstream water depth;
y_2 = water depth at vena contracta;
y_3 = downstream water depth;
α_j = velocity distribution coefficient;
δ = contraction coefficient (ratio of minimum depth y_j to gate opening w);
θ = angle of the gate lip;
ξ = energy loss coefficient; and
ρ = density of water (mass per unit volume).

References

Bos, M. G., ed. (1989). *Discharge measurement structures*, 3rd Ed., Publication 20, International Institute for Land Reclamation and Improvement/ILRI, Wageningen, The Netherlands.

Bos, M. G., Replogle, J. A., and Clemmens, A. J. (1984). *Flow measuring flumes for open channel systems*, Wiley, New York.

Buyalski, C. P. (1983). *Discharge algorithms for canal radial gates*, REC-ERC-83-9, Engineering and Research Center, U.S. Bureau of Reclamation, Denver.

Clemmens, A. J., Wahl, T. L., Bos, M. G., and Replogle, J. A. (2001). *Water measurement with flumes and weirs*, Publication #58, International Institute for Land Reclamation and Improvement, Wageningen, The Netherlands.

Fangmeier, D. D., and Strelkoff, T. S. (1968). ''Solutions for gravity flow under sluice gates.'' *J. Eng. Mech. Div., Am. Soc. Civ. Eng.*, 94(1), 153–176.

Gunal, M., and Narayanan, R. (1996). ''Hydraulic jump in sloping channels.'' *J. Hydraul. Eng.*, 122(8), 436–442.

Henderson, F. M. (1966). *Open channel flow*, The Macmillan Company, New York.

Henry, H. (1950). ''Discussion: Diffusion of submerged jet.'' *Trans. Am. Soc. Civ. Eng.*, 115, 687–697.

Isaacs, L. T., and Allen, P. H. (1994). ''Contraction coefficients for radial sluice gates.'' *Proc. 1994 Int. Conf. on Hydraulics in Civil Engineering, National Conf. Publ. No. 94/1*, Institute of Engineers, Barton, ACT, Australia, 262–265.

Montes, J. S. (1997). ''Irrotational flow and real fluid effects under planar sluice gates.'' *J. Hydraul. Eng.*, 123(3), 219–232.

Montes, J. S. (1999). ''Closure to 'Irrotational flow and real fluid effects under planar sluice gates'.'' *J. Hydraul. Eng.*, 125(2), 212–213.

Narayanan, R. (1975). ''Wall jet analogy to hydraulic jump.'' *J. Hydraul. Div., Am. Soc. Civ. Eng.*, 101(3), 347–359.

Rajaratnam, N. (1965a). ''Submerged hydraulic jump.'' *J. Hydraul. Div., Am. Soc. Civ. Eng.*, 91(4), 71–96.

Rajaratnam, N. (1965b). ''The hydraulic jump as a wall jet.'' *J. Hydraul. Div., Am. Soc. Civ. Eng.*, 91(5), 107–132.

Rajaratnam, N., and Subramanya, K. (1967a). ''Flow Immediately below submerged sluice gate.'' *J. Hydraul. Div., Am. Soc. Civ. Eng.*, 93(4), 57–77.

Rajaratnam, N., and Subramanya, K. (1967b). ''Flow equations for sluice gate.'' *J. Irrig. Drain. Div., Proc., ASCE*, 93(IR3), 167–186.

Replogle, J. A. (1975). ''Critical flow flumes with complex cross-section.'' *Irrigation and drainage in an age of competition for resources, ASCE Specialty Conf. Proc.*, New York, 366–388.

Rouse, H., Siao, T. T., and Nagaratnam, S. (1959). ''Turbulence characteristics of the hydraulic jump.'' *Trans. Am. Soc. Civ. Eng.*, 124, 926–966.

Speerli, J., and Hager, W. H. (1999). ''Discussion: Irrotational flow and real fluid effects under planar sluice gates.'' *J. Hydraul. Eng.*, 125(2), 208–210.

Swamee, P. K. (1992). ''Sluice-gate discharge equations.'' *J. Irrig. Drain. Eng.*, 118(1), 56–60.

Tel, J. (2000). ''Discharge relations for radial gates.'' MSc thesis, Delft Technical Univ., Delft, The Netherlands.

Toch, A. (1955). ''Discharge characteristics of Tainter gates.'' *Trans. Am. Soc. Civ. Eng.*, 120, 290–300.

von Helmholtz, H. L. (1868). ''Ueber diskontinuirliche Flussigkeitbewegungen.'' *Monatsberichten der Königlich Pressischen Akademie der Wissenschaften zu Berlin*, Berlin, Germany, 215–228 (in German).

Webby, M. G. (1999). ''Discussion: Irrotational flow and real fluid effects under planar sluice gates.'' *J. Hydraul. Eng.*, 125(2), 210–212.